Sol-Gel Synthesis and Spectral Characterizations of (35-x)B₂O₃-65Bi₂O₃-x Fe₂O₃ Glass System

Rajesh Kumar Sharma[*] and V. Vaijayanthi

Department of Chemistry, Kanchi Mamunivar Centre for P.G. Studies, Pondicherry-605008, India

*Corresponding author: E-mail: rksepr@gmail.com

Sol-gel technique was used to prepare glasses of the $(35\text{-}x)B_2O_3\text{-}65Bi_2O_3\text{-}x\ Fe_2O_3$ $(0.1 \leq x \leq 0.4)$ system (A1-A4: x = 0.1, 0.2, 0.3, 0.4). The local structure and symmetry around trivalent iron were determined by studying X-band powder EPR spectra at room temperature. The EPR spectra of trivalent iron in glass samples are characterized by a more intense line at g = 4.2 and a less intense line at g = 2.0. The EPR line at g = 4.2 is attributed to trivalent iron in rhombic octahedral environment. The line at g = 2.0 is because of two or more trivalent iron coupling through dipole-dipole interactions in distorted octahedral symmetry. The intensity of EPR lines is dependent of Fe_2O_3 content in the glass samples. At higher concentration of Fe_2O_3, EPR line at g = 4.2 is less intense whereas the line at g = 2.0 is more intense which is ascribed to the formation of clusters of trivalent iron. The electronic spectra of glass samples show two broad bands corresponding to *d-d* transition in the range 410-450 nm and in the range 530-570 nm, respectively which are assigned to trivalent iron in distorted octahedral environment.

Keywords: Glass samples, Sol-gel technique, Dipole-dipole interaction, Electronic spectra.

INTRODUCTION

During recent years, there has been an enormous interest in the studies of transition metal oxide glasses because of their important technological uses in electrochemical, electronics, tunable solid state lasers and optical telecommunication [1-5]. Fe_2O_3 forms a potential component for the formation of glasses by sol-gel technique [6]. Glasses containing Fe_2O_3 are relatively less studied on account of high melting point of Fe_2O_3. Bi_2O_3 is not a good glass network former because of relatively small amount of field strength (0.53) of Bi^{3+} ion. But in the presence of B_2O_3 as a glass former, glasses are produced over a large range of compositions. Inorganic glasses like silicate, borate, phosphate, germinate, tellurite containing trivalent iron ions have been extensively studied by electron paramagnetic resonance spectroscopy [7-9].

Trivalent and divalent states of iron occupy different environments. Trivalent irons are present in both tetrahedral and octahedral symmetry whereas divalent irons prefer to be in octahedral environments only. EPR lines at g = 4.2 and = 2.0 for trivalent iron $(3d^5, {}^6A_{1g})$ are observed due to transitions inside Kramers' doublets. Divalent iron ions $(3d^6)$ show high magnetic aniso-

tropy due to strong interaction by L-S coupling whereas trivalent iron ions $(3d^5)$ show small amount of magnetic anisotropy because of its zero orbital angular momentum (L = 0). The EPR and electronic spectra together are employed to find out the local structure and spatial distribution of trivalent iron in the glass samples. The calculated g-values from EPR spectra do not depend on the composition of glass samples which indicate that the symmetry around trivalent iron is unchanged. In the present work, we study structure-property relations in glasses by means of XRD patterns, EPR and electronic spectra.

EXPERIMENTAL

Four glass samples of compositions $(35\text{-}x)B_2O_3\text{-}65Bi_2O_3\text{-}x\ Fe_2O_3$ $(0.1 \leq x \leq 0.4)$ were prepared by sol-gel process using reagent grade chemicals. The 0.05 M solutions of iron(III) nitrates, bismuth(III) nitrate and boric acid were prepared by taking their calculated amounts. The sol was prepared by mixing these solutions with 25 mL of 2 M citric acid solution. The gel was prepared by heating the resulting sol at ~ 333 K. The gel thus formed is then heated at ~ 393 K. These dried gels are heated in silica crucibles placed in an electrically heated furnace for

about 30 min to prevent volatilization and melted in the range 1313-1374 K and the melt was further maintained at this temperature for 0.5 h. The melts were then quickly poured on an ice cold aluminium plate and air quenched by pressing under another ice cold aluminium plate. The prepared glass samples were stored in a dessicator to prevent further degradation. The glass samples are grounded into fine powders to study their properties.

The glassy phase was ascertained by powder XRD patterns recorded using a Seifert diffractometer (model XRD 3000) with CuKα radiation (λ = 1.54056 Å). The EPR spectra of samples were recorded on a JEOL JES TE100 EPR spectrometer operating at X-band frequency having a 100 kHz field modulation to obtain first derivative spectra at room temperature. The electronic spectra of glass samples were recorded in UV-visible region on Varian Cary 5000 UV-visible NIR spectrophotometer at room temperature in the wave length range of 400-650 nm.

RESULTS AND DISCUSSION

Powder XRD patterns of samples A1-A4 are presented in Fig. 1. Powder XRD patterns show a broad peak around 2θ value of 30º which disappears at higher diffraction angle confirms the amorphous nature of prepared samples. The room temperature X-band powder electron paramagnetic resonance spectra of $(35-x)B_2O_3-65Bi_2O_3-x$ Fe_2O_3 $(0.1 \le x \le 0.4)$ glass system are shown in Fig. 2. EPR spectra of trivalent iron in high spin configuration have been thoroughly studied in an octahedral environment. The ground state for high spin trivalent iron ions is $^6S_{5/2}$ ($^6A_{1g}$). The observed g-value in EPR spectra should be 2.0023 (free electron value) because of zero L (resultant orbital angular momentum) value for $3d^5$ in high spin configuration [10]. The observed g-values, 4.2 and 2.0 in glass samples are characteristics of trivalent iron in distorted octahedral environment. EPR spectra of trivalent iron in high spin configuration are studied by Zeeman effect and zero field splitting (ZFS).
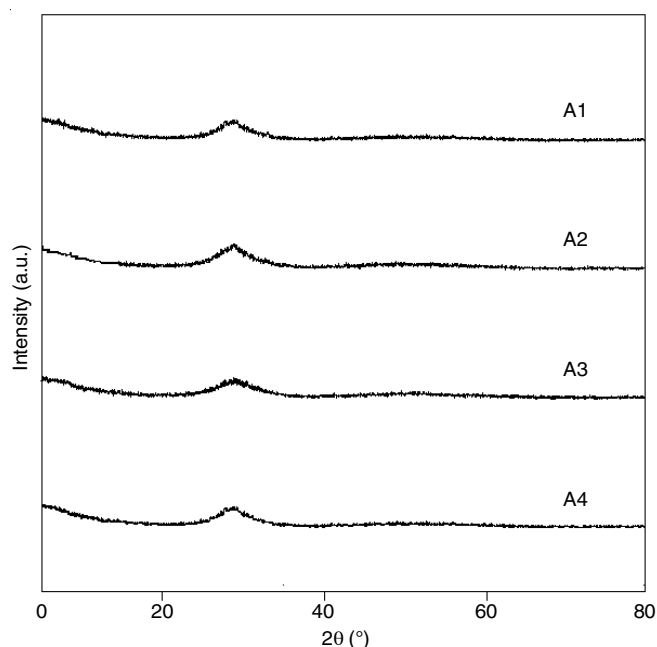

Fig. 1. Powder XRD patterns of $(35-x)B_2O_3-65Bi_2O_3-x$ Fe_2O_3 $(0.1 \le x \le 0.4)$ glasses
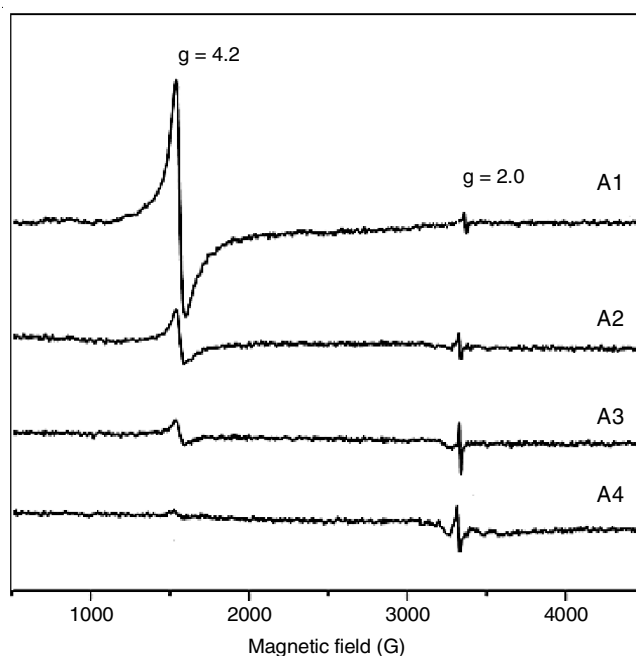
Fig. 2. X-band powder EPR spectra of $(35-x)B_2O_3-65Bi_2O_3-x$ Fe_2O_3 $(0.1 \le x \le 0.4)$ glasses at room temperature

In the absence of magnetic field, zero-field splitting removes the spin degeneracy of trivalent iron ions ($3d^5$) in high spin configuration. The X-band powder EPR spectra of trivalent iron in high spin configuration can be explained by the following spin-Hamiltonian [11]:

$$H = g \beta_e H S + D [S_z^2 - 35/12] + E (S_x^2 - S_y^2) + A S I + 1/6 a [S_x^4 + S_y^4 + S_z^4 - 707/16] + 1/180 F [35 S_z^4 - 475/2 S_z^2 + 3255/16] \quad (1)$$

where S, H and β_e are resultant spin (s = 5/2), magnetic field and Bohr magneton, respectively. The terms $D[S_z^2-35/12]$ and $E(S_{x2}-S_y^2)$ in the above equation are axial and rhombic components of the crystal field, respectively. If D = E = 0, it shows a free trivalent iron in magnetic field (H). When E = 0, it indicates an axial crystal field. Rhombic character increases with the increase in λ = E/D [12]. In trivalent iron with small tetragonal distortion, D ≤ hν and E = 0 due to the enormously low spin-orbit coupling, g-values are very close to 2.0. Due to this fact EPR spectra are observed at room temperature. If D ≥ hν and λ =1/3, g-value from the middle Kramers' doublet is close to 4.2. The g-value from the EPR spectra of trivalent iron in silicate, borate, phosphate and sulphate glasses was found to be 4.2. Kramers' rule [11,13] states if an ion has an odd number of electrons, the degeneracy of every level must remain at least twofold in the absence of a magnetic field. According to Kramers' rule the spin degeneracy of every level of trivalent iron ($3d^5$) is doubly degenerate. Zero field splitting (ZFS) produces three Kramers' doublets, |± 5/2 >, |± 3/2 > and |± 1/2 > for trivalent iron in high spin configuration. The EPR line at g = 2.0 corresponds to the transition from the |± 1/2 > doublet [14] and the absorption line [15] at g = 4.2 arises due to the transition from the |± 3/2 > doublet.

EPR line shapes [12] of trivalent iron in glass samples are represented by an intense, well defined EPR line at g = 4.2 and relatively less intense lines at g = 2.0 and 6.0 or 10.0 of which,

the commonly encountered cases are the combination of g = 4.2 and 2.0 [16]. EPR lines [16] at g = 4.2 and 2.0 do not show coordination number for trivalent iron and it was proposed that the line at g = 4.2 may arise either in distorted octahedral or in distorted tetrahedral environment. The above idea was explained on the basis of group theoretical considerations [10]. The study of EPR spectra of trivalent iron in biological systems [17] has also revealed that lines at g = 4.2 and 2.0 arise in distorted octahedral environment. The results of EPR studies in various glasses show that the EPR absorption lines [18,19] at g value of 4.2 and 2.0 arise from trivalent iron in distorted octahedral environment. In (35-x)B$_2$O$_3$-65Bi$_2$O$_3$-x Fe$_2$O$_3$ glass samples, the EPR lines at g = 4.2 have been ascribed to the remote trivalent iron in octahedral symmetry having rhombic character [19] and the EPR lines at g = 2.0 are attributed to the formation of clusters of two or more paramagnetic trivalent iron which interacted by dipolar coupling in a distorted octahedral symmetry [20]. The observed g-values from EPR spectra do not depend on the composition of glass samples which shows that symmetry and spatial distribution around trivalent iron are identical. The intensity of EPR lines depend on the composition of glass samples. At higher concentration of Fe$_2$O$_3$, remote trivalent irons assemble to form clusters [20] and the characteristic structural units are less represented due to the complete removal of the nearby trivalent iron in the glass samples. This may be the reason for less intense EPR line at g= 4.2 and more intense EPR line at g= 2.0.

The results of EPR studies of glass system revealed that trivalent iron are in a distorted octahedral environment. The electronic spectra of (35-x)B$_2$O$_3$-65Bi$_2$O$_3$-x Fe$_2$O$_3$ glass samples is presented in Fig. 3.
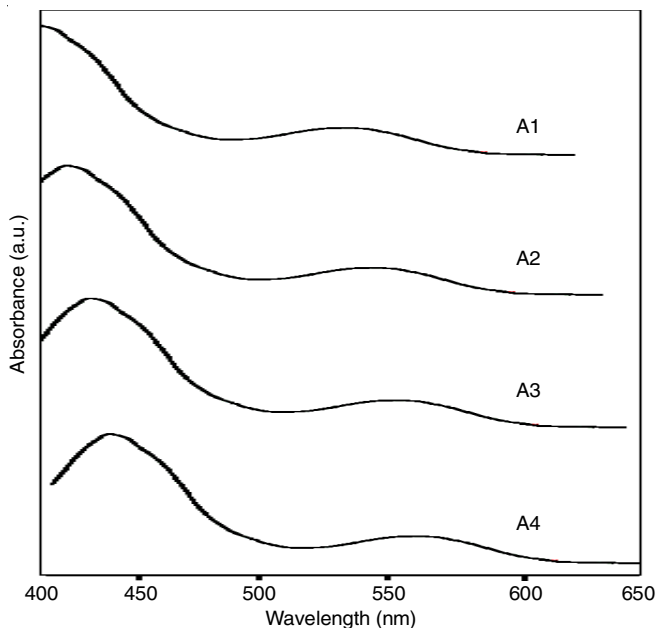
Fig. 3.   Electronic spectra of (35-x)B$_2$O$_3$-65Bi$_2$O$_3$-x Fe$_2$O$_3$ (0.1 ≤ x ≤ 0.4) glasses at room temperature

There are no spin-allowed transitions for trivalent iron (^{6}A$_{1g}$) in high spin configuration and all transitions are not only Laporte forbidden but also spin forbidden. In excited state, trivalent iron ions in a weak crystal field provide quartet terms ^{4}G, ^{4}D, ^{4}P and ^{4}F and doublet terms. ^{4}G is the lowest excited

term from quartet terms. The states arising from these quartet terms in a strong octahedral crystal field are ^{4}G → ^{4}A$_{1g}$, ^{4}E$_g$, ^{4}T$_{1g}$, ^{4}T$_{2g}$; ^{4}P → ^{4}T$_{1g}$; ^{4}F → ^{4}A$_{2g}$, ^{4}T$_{1g}$, ^{4}T$_{2g}$ and ^{4}D → ^{4}E$_g$, ^{4}T$_{2g}$. A schematic energy level diagram of trivalent iron ($3d^5$) showing only quartet terms is presented in Fig. 4. Spin-forbidden transitions take place between two different states because the degeneracy of the terms is not lifted by first-order crystal field perturbation [21] in a weak crystal field. In the electronic spectra of trivalent iron in glass samples, spin-forbidden electronic transitions take place between ground state and quartet states but the transitions from the ground to doublet states are too weak to be observed. In the present work, one broad intense absorption d-d band corresponding to the transition ^{6}A$_{1g}$(S) → ^{4}T$_{2g}$(G) is identified in A1.
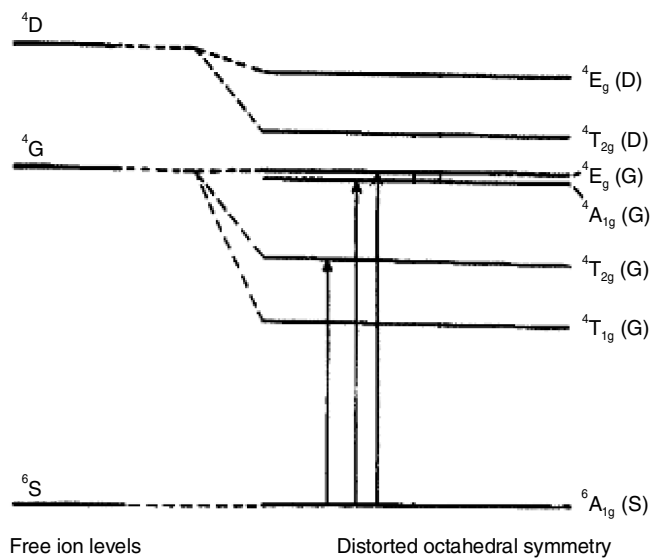

Fig. 4. Energy diagram for d^5 configuration showing only quartet terms

Two d-d bands are observed in samples A2-A4 which are ascribed to the transition ^{6}A$_{1g}$(S) → ^{4}T$_{1g}$(G), ^{4}E$_g$ (G) in range 410-440 nm (24390-22215 cm^{-1}) and another broad d-d band is identified corresponding to the transition ^{6}A$_{1g}$(S) → ^{4}T$_{2g}$(G) in the range 530-570 nm (18868-17544 cm^{-1}). The observed two d-d bands in the glass samples are characteristics of trivalent iron [9,22-24] in distorted octahedral environment.

Conclusion

The results of X-band powder electron paramagnetic resonance spectra of studied glasses show more intense line at g = 4.2 and less intense line at g = 2.0, which are characteristic of trivalent iron. The EPR lines at g = 4.2 are ascribed to the remote trivalent iron in octahedral symmetry having rhombic distortion whereas the absorption lines at g = 2.0 are attributed to the formation of clusters of trivalent iron ions. The calculated g-values do not depend on the composition of glass samples which shows that the symmetry around trivalent iron is identical. The intensity of EPR lines at g = 4.2 and g = 2.0 are dependent of Fe$_2$O$_3$ content. At higher Fe$_2$O$_3$ content, EPR line at g = 4.2 is less intense whereas the line at g = 2.0 is more intense. The electronic spectra of glasses have revealed that trivalent iron exhibits two bands corresponding to d-d transition in a distorted octahedral environment.

CONFLICT OF INTEREST

The authors declare that there is no conflict of interests regarding the publication of this article.

REFERENCES

1. A.K. Yadav and P. Singh, *RSC Adv.*, **5**, 67583 (2015);
    https://doi.org/10.1039/C5RA13043C.
2. R.K. Brow, T.M. Alam, D.R. Tallant and R.J. Kirkpatrick, *MRS Bull.*, **23**, 63 (1998);
    https://doi.org/10.1557/S088376940003102X.
3. D.W. Hall, M.A. Newhouse, N.F. Borelli, W.H. Dumbaugh and D.L. Weidman, *Appl. Phys. Lett.*, **541**, 1293 (1989);
    https://doi.org/10.1063/1.100697.
4. D. Lezal, J. Pedlikova, P. Kostka, J. Bludska, M. Poulain and J. Zavadil, *J. Non-Crystall. Solids*, **284**, 288 (2001);
    https://doi.org/10.1016/S0022-3093(01)00425-2.
5. M. Jamnický, P. Znásik, D. Tunega and M.D. Ingram, *J. Non-Cryst. Solids*, **185**, 151 (1995);
    https://doi.org/10.1016/0022-3093(94)00642-3.
6. Z. Yue, L. Li, J. Zhou, H. Zhang and Z. Gui, *Mater. Sci. Eng. B*, **64**, 68 (1999);
    https://doi.org/10.1016/S0921-5107(99)00152-X.
7. R.P. Sreekanth Chakradhar, B. Yasoda, J.L. Rao and N.O. Gopal, *Mater. Res. Bull.*, **41**, 1646 (2006);
    https://doi.org/10.1016/j.materresbull.2006.02.028.
8. W.M. Bergo, W.M. Pontuschka and J.M. Prison, *Mater. Chem. Phys.*, **108**, 142 (2008);
    https://doi.org/10.1016/j.matchemphys.2007.09.021.
9. R.S. Muralidhara, C.R. Kesavulu, J.L. Rao, R.V. Anavekar and R.P.S. Chakradhar, *J. Phys. Chem. Solids*, **71**, 1651 (2010);
    https://doi.org/10.1016/j.jpcs.2010.09.013.
10. D. Loveridge and S. Parke, *Phys. Chem. Glasses*, **12**, 19 (1971).
11. R.S. Drago, Physical Methods for Chemists, Affiliated East-West Press Private Limited: New Delhi, edn 2, p. 559, 583 (1965).
12. K.J. Rao and B.G. Rao, *Proc. Indian Acad. Sci. Chem. Sci.*, **95**, 169 (1985).
13. J.A. Weil, J.R. Bolton and J.E. Wertz, Electron Paramagnetic Resonance: Elementary Theory and Practical Applications, John Wiley & Sons, Inc.: New York, p. 220 (1994).
14. J.R. Pilbrow, Transition Ion Electron Paramagnetic Resonance, Clarendon: Oxford, p. 136 (1990).
15. T. Castner Jr., G.S. Newell Jr., W.C. Holton and C.P. Slichter, *J. Chem. Phys.*, **32**, 668 (1960);
    https://doi.org/10.1063/1.1730779.
16. C.R. Kurkjan and E.A. Sigety, *Phys. Chem. Glasses*, **9**, 73 (1968).
17. R.G. Schulman and W.M. Walsh Jr., *Bull. Am. Phys. Soc.*, **8**, 199 (1963).
18. D.W. Moon, A.J.M. Aitken, R.K. McCrone and C.S. Cieloszyk, *Phys. Chem. Glasses*, **16**, 91 (1975).
19. D.L. Griscom, *J. Non-Cryst. Solids*, **40**, 211 (1980);
    https://doi.org/10.1016/0022-3093(80)90105-2.
20. I. Ardelean, P. Pascuta and L.V. Giurgiu, *Int. J. Mod. Phys. B*, **17**, 3049 (2003);
    https://doi.org/10.1142/S0217979203020648.
21. D.N. Sathyanarayana, Electronic Abssorption Spectroscopy and Related Technoques, Universities Press Limited, Hyderabad, India, p. 282 (2001).
22. T. Bates, ed.: J.D. Mackenzie, Modern Aspects of the Vitreous State, Butterworths, London, p. 242 (1962).
23. T. Abritta and F. de Souza Barros, *J. Lumin.*, **40-41**, 187 (1988);
    https://doi.org/10.1016/0022-2313(88)90150-0.
24. G. Giridhar, D. Punyaseshudu, M.V.V.K. Srinivas Prasad, M. Venkateswarlu and G. Srinivas, *Acta Phys. Pol. A*, **123**, 761 (2013);
    https://doi.org/10.12693/APhysPolA.123.761.